Algorithms Theoretical Basis Document for the Low Earth Orbiter Sea Surface Temperature Processing

GLB SST (OSI-201-b, OSI-201-c)
NAR SST (OSI-202-c, OSI-202-d)
MGR SST (OSI-204-b , OSI-204-c)

Version: 1.8
Date: 9/7/2020

S. Saux Picart

Documentation change record

Version	Date	Authors	Description
1_0	26/11/2014	M-F/CMS	Initial version, submitted to EUMETSAT
1_1	11/02/2014	M-F/CMS	Updated version, taking into account RIDs from Product Consolidation Review: • Introduction has been updated in response to [df01, df03, AOC1]. In particular products are now described and scientific motivations have been added. • [df02] has been answered by adding reference to PRD 3.0 • Section 2.5 (Ancillary data) and 2.6 (Computing and programming considerations) were added in response to [AOC1] • [AOC3]: It has been made clear in the introduction that any mention of SST refer to sub-skin SST unless otherwise stated. A reference to the sub-skin-to-skin temperature conversion factor has been added in section 3.4.1. • [AOC4]: The use of the term "error" has been improved throughout the text. • [AOC5, AOC6]: Information has been added to section 2.4 on SSES. • [AOC7, JA − 07]: More detail are given about the smoothing procedure in section 3.3.5. • Section 3.4.2 has been modified to incorporate modification and correction suggested by [AOC8, JA-09, OE2] • [AOC9]: Section 4.1 has been developed in particular to include example of control graphs. • [JA − 01]: Section 2.2.2 has been updated to include information about how we deal with the 3A/3B channel switch in twilight conditions. • [JA − 02]: A table describing the indicators has been added to section 2.3. • Figure 3 and 4 have been updated as per recommendation [JA-05] • Other typos and minor modifications have been dealt with as per other RIDs

Version	Date	Authors	Description
1_2	20/11/2015	M-F/CMS	Minor error corrected in the coefficient of tables 6 and 7
1_3	28/6/2018	M-F/CMS	Upcoming upgrade of GBL SST and MGR SST planned in July 2018: • Upgrade of cloud mask. MAIAv3 to MAIAv4 • Upgrade of GBL SST: more importance is given to the quality level over the proximity in time and space
1_4	28/6/2018	M-F/CMS	Upgrade of the processing to ingest NOAA-20 data (instead of NPP data) and produce NAR product (OSI-202-c) accordingly.
1_5	28/3/2019	M-F/CMS	Minor corrections suggested by reviewers.
1_6	6/5/2020	M-F/CMS	Adding Metop-C related information for ORR.
1_7	20/6/2020	M-F/CMS	Minor modifications following reviewers comments.
1_8	9/7/2020	M-F/CMS	Modification of NOAA-20 SST algorithm coefficients.

Contents

1 Introduction **5**
1.1 Scope of the document . . . 5
1.2 Reference documents . . . 5
1.3 Applicable documents . . . 5
1.4 Scientific motivations . . . 5
1.5 Characteristics of the instruments . . . 6
1.5.1 Metop/AVHRR . . . 6
1.5.2 JPSS/VIIRS . . . 7
1.6 Acronyms and definitions . . . 7

2 Low Earth Orbiter processing chain overview **9**
2.1 Products . . . 9
2.2 SST computation in the new LEO processing chain . . . 10
2.2.1 Land/Lake/Sea/Ice/Cloud mask . . . 10
2.2.2 The "classical" SST computation . . . 11
2.2.3 Bias correction Overview . . . 11
2.3 Quality level and test indicators . . . 11
2.4 Sensor Specific Error Statistics (SSES) . . . 13
2.5 Ancillary data . . . 14

3 Low Earth Orbiter processing chain algorithms descriptions **15**
3.1 Saharan Dust Index (SDI) . . . 15
3.2 Ice detection algorithm . . . 15
3.3 SST algorithms . . . 15
3.4 Non-linear SST algorithm . . . 15
3.5 Bias correction . . . 17
3.5.1 Simulation of brightness temperature . . . 17
3.5.2 Adjustment of the BTs . . . 18
3.5.3 Corrected SST . . . 19

4 SST temporal synthesis **21**

5 Validation procedure **23**
5.1 The Matchup Dataset . . . 23
5.2 Validation results . . . 23

List of Figures

1 Channels of VIIRS instrument. From Lee et al. (2006), BAMS. 7
2 LEO processing chain overview. 9
3 Schematic of the SST processing (including bias correction) in the LEO SST chain. 10
4 RTTOV simulations of brightness temperature for 10.8 and 12.0μm for a sample granule. 18
5 Sample global BT adjustment field for 10.8μm channel. 20
6 Average (JFM 2012) difference between "classical" SST and guess SST (top), and difference between "simulated" SST and guess SST (bottom), this is the predicted SST uncertainty or average estimated algorithm uncertainty. Note that these results have been obtained for Metop-A/AVHRR. 21
7 Sample of the routine validation maps that can be found on http://osi-saf.eumetsat.int. Monthly map of the mean bias (top) and standard deviation (bottom) of satellite SST minus drifting buoys temperature measurement, April 2018. 24

List of Tables

1 Channels of AVHRR instrument. 6
2 List of indicators contributing to the quality level 12
3 SSES for METOP-B SST 13
4 SSES for METOP-C SST 14
5 List of ancillary data needed 14
6 Coefficient of the algorithm for Metop-B/AVHRR. 16
7 Coefficient of the algorithm for Metop-C/AVHRR. 16
8 Coefficient of the algorithm for NOAA-20/VIIRS. 17

1 Introduction

1.1 Scope of the document

The EUMETSAT Satellite Application Facilities (SAFs) are dedicated centres of excellence for processing satellite data. They form an integral part of the distributed EUMETSAT Application Ground Segment. The Ocean and Sea Ice SAF, led by Météo-France/Centre de Météorologie Spatiale (M-F/CMS), has the responsibility of developing, validating and distributing products of Sea Surface Temperature (SST), radiative fluxes, wind and Sea Ice for a variety of platforms/sensors. More information can be found at http://osi-saf.eumetsat.int. The scope of this document is to describe the algorithms implemented in the development of the processing chain for Metop/Advanced Very High Resolution Radiometer (AVHRR) and Joint Polar Satellite System/Visible Infrared Imaging Radiometer Suite (JPSS/VIIRS) SST. This chain is delivering the four following products (see [AD.1] for more information about these products):

- OSI-201-b: Global Metop Sea Surface Temperature from Metop-B (Metop01)
- OSI-201-c: Global Metop Sea Surface Temperature from Metop-C (Metop03)
- OSI-202-c: North Atlantic Regional Sea Surface Temperature from Metop-B (Metop01) and NOAA-20 (JPSS-1)
- OSI-202-d: North Atlantic Regional Sea Surface Temperature from Metop-C (Metop03) and NOAA-20 (JPSS-1)
- OSI-204-b: Full resolution Metop Sea Surface Temperature metagranules from Metop-B (Metop01)
- OSI-204-c: Full resolution Metop Sea Surface Temperature metagranules from Metop-C (Metop03)

1.2 Reference documents

Ref	Title	Code
[RD.1]	MAIA version 4 for Suomi SNPP-VIIRS and NOAA/METOP-AVHRR cloud mask and classification – Scientific user manual.	NWPSAF-MF-UD-009
[RD.2]	Global Sea Ice Edge and Type - Algorithm Theoretical Basis Document	SAF/OSI/CDOP2/MET-Norway/SCI/MA/208
[RD.3]	RTTOV v11 Users Guide.	NWPSAF-MO-UD-028
[RD.4]	RTTOV-11 Science and validation report.	NWPSAF-MO-TV-032
[RD.5]	Validation report for OSI SAF Metop/AVHRR SST. OSI-201-b / OSI-202-b / OSI-204-b	SAF/OSI/CDOP2/M-F/SCI/TEC/234
[RD.6]	Scientific Validation Report for the Low Earth Orbiter Satellite Sea Surface Temperature. OSI-201-c, OSI-202-c, OSI-204-c	SAF/OSI/CDOP3/ MF/SCI/RP/382

1.3 Applicable documents

Ref	Title	Code
[AD.1]	OSI SAF CDOP 3, Product Requirement Document version 1.4	SAF/OSI/CDOP3/MF/MGT/PL/2-001

Channel	wavelength interval (μm)
1	0.58 - 0.68
2	0.725 - 1.00
3A (6)	1.58 - 1.64
3B	3.55 - 3.93
4	10.3 - 11.3
5	11.5 - 12.5

Table 1: Channels of AVHRR instrument.

1.4 Scientific motivations

The retrieval of SST from infrared radiometric measurements is a topic in constant evolution. Most methods however are declinations of the Multichannel SST algorithm (McCain et al., 1985) and the Nonlinear SST algorithm (Walton et al., 1998). Algorithms to compute SST from remote sensing infrared Brightness Temperatures (BT) perform relatively well and are very simple to implement (providing all necessary pre-processing such as cloud, ice, land masking and so on). However when applied globally on long time series they reveal anomalies, in particular regional and seasonal biases when compared to drifting buoys measurements (Merchant et al., 2009; Le Borgne et al., 2012). Two approaches have been developed to correct for these biases: the Optimal Estimation method designed by Merchant et al. (2008) and the bias correction method designed by Le Borgne et al. (2011). They both rely on the use of simulations from a numerical weather prediction model and an atmospheric Radiative Transfer Model (RTM). Such methods make the best of the knowledge of the atmospheric condition (temperature, T and water vapour profiles, q) given by NWP models in order to improve SST. Up to now, bias correction scheme is not applied for the production of OSI-SAF Low Earth Orbiter (LEO) SST products which therefore contain regional and seasonal biases. We have chosen to implement the bias correction scheme designed by Le Borgne et al. (2011). The motivation for this upgrade of the current LEO SST processing chain lays in the potential enhancement of the quality of the products.

1.5 Characteristics of the instruments

The LEO SST processing chain currently process data from two instruments which characteristics are given here.

1.5.1 Metop/AVHRR

The AVHRR instrument has been in operation since 1978 on the US NOAA Polar-Orbiting Environmental Satellite. It also flies on the METOP satellites of the EUMETSAT Polar System program since 2006.

The version of the AVHRR instrument flying on METOP satellites is the AVHRR/3. It performs radiometric measurements in six channels: Three in the visible/near infrared region of the spectrum (Channel 1, 2 and 3A) and three in the atmospheric window of the infrared spectrum (listed in Table 1). Only five channels out of the six are transmitted to the ground at any given time: Channel 3A (also called Channel 6) is transmitted during daytime and is replaced by Channel 3B at night.

AVHRR has a resolution of 1.1 km at nadir; its swath is approximately 2500km. Metop satellites follow sun-synchronous orbits at an altitude of about 800km above the Earth. Each orbit is about 100 minutes long and transmitted to the ground as granules of 3 minutes of acquisition.

1.5.2 JPSS/VIIRS

The VIIRS instrument is following the legacy of the AVHRR on NOAA and MODIS Aqua and Terra satellites. It is currently flying on S-NPP and NOAA-20 (the first flight unit of JPSS programme). In the context of OSI SAF NOAA-20/VIIRS data are being processed in the continuity of S-NPP/VIIRS data. VIIRS is operating in 22 imaging and radiometric bands covering wavelengths from 0.41 to 12.5 microns (see figure 1).

Table 1. VIIRS channels.

Band number/gain	VIIRS wavelength (μm)	VIIRS nadir pixel size along track × cross track (km)	Primary application
M1, dual	0.412	0.742 × 0.259	Ocean color, aerosols
M2, dual	0.445	0.742 × 0.259	Ocean color, aerosols
M3, dual	0.488	0.742 × 0.259	Ocean color, aerosols
M4, dual	0.555	0.742 × 0.259	Ocean color, aerosols
I1, single	0.640	0.371 × 0.387	Imagery, vegetation
M5, dual	0.672	0.742 × 0.259	Ocean color, aerosols
M6, single	0.746	0.742 × 0.776	Atmospheric correction
I2, single	0.865	0.371 × 0.387	Vegetation
M7, dual	0.865	0.742 × 0.259	Ocean color, aerosols
DNB, multiple	0.7	0.742 × 0.742	Imagery
M8, single	1.24	0.742 × 0.776	Cloud particle size
M9, single	1.38	0.742 × 0.776	Cirrus cloud cover
M10, single	1.61	0.742 × 0.776	Snow fraction
I3, single	1.61	0.371 × 0.387	Binary snow map
M11, single	2.25	0.742 × 0.776	Clouds
M12, single	3.70	0.742 × 0.776	Sea surface temperature (SST)
I4, single	3.74	0.371 × 0.387	Imagery, clouds
M13, dual	4.05	0.742 × 0.259	SST, fires
M14, single	8.55	0.742 ×0.776	Cloud-top properties
M15, single	10.76	0.742 × 0.776	SST
I5, single	11.45	0.371 × 0.387	Cloud imagery
M16, single	12.01	0.742 × 0.776	SST

Figure 1: Channels of VIIRS instrument. From Lee et al. (2006), BAMS.

VIIRS has a spatial resolution of 750m in the IR channels used for SST retrieval; its swath is about 3000km. NOAA-20 is following a sun-synchronous orbit at an altitude of 825km. The equatorial crossing time is 13:25 in ascending leg.

1.6 Acronyms and definitions

The term workfile is used to designate intermediary files produced by the processing chain. Workfiles contains most of the intermediate variables of the processing.

AOD	Aerosol Optical Depth
AVHRR	Advanced Very High Resolution Radiometer
BT	Brightness Temperature
ECMWF	European Centre for Medium-range Weather Forecasts
GDS	GHRSST Data Specification
GHRSST	Group for High Resolution SST
GTS	Global Telecommunication System

IR	Infrared
JPSS	Joint Polar Satellite System
LEO	Low Earth Orbiter
M-F/CMS	Météo-France/Centre de Météorologie Spatiale
MDS	Matchup DataSet
MSG	Meteosat Second Generation
Metop	Meteorological Operational
NAR	North Atlantic Regional
NAAPS	Navy Aerosol Analysis and Prediction System
NSIDC	National Snow and Ice Data Center
NWP SAF	Numerical Weather Prediction Satellite Application Facility
OSI SAF	Ocean and Sea Ice Satellite Application Facility
OSTIA	Operational Sea Surface Temperature and Sea Ice Analysis
QL	Quality Level
RTM	Radiative Transfer Model
RTTOV	Radiative Transfer for TOVS
SAF	Satellite Application Facility
SDI	Saharan Dust Index
SEVIRI	Spinning Enhanced Visible and InfraRed Imager
SNPP	Suomi National Polar-Orbiting Partnership
SSES	Sensor Specific Error Statistics
SST	Sea Surface Temperature
SZA	Sun Zenith Angle
TIROS	Television Infrared Observation Satellite
TOVS	TIROS Operational Vertical Sounder
VIIRS	Visible Infrared Imaging Radiometer Suite

2 Low Earth Orbiter processing chain overview

This section gives an overview of the general functioning of the new processing chain for Low Earth Orbiter SST retrieval. The computation of SST is performed for all non-cloudy sea or lake pixels regardless of other consideration about the conditions of measurements and the algorithms used. The related uncertainties are evaluated and summarised by the quality level. The quality level is itself a concatenation of many indicators which ensure that each potential problem is taken into account and quantified throughout the whole process (for more information, see section 2.3).

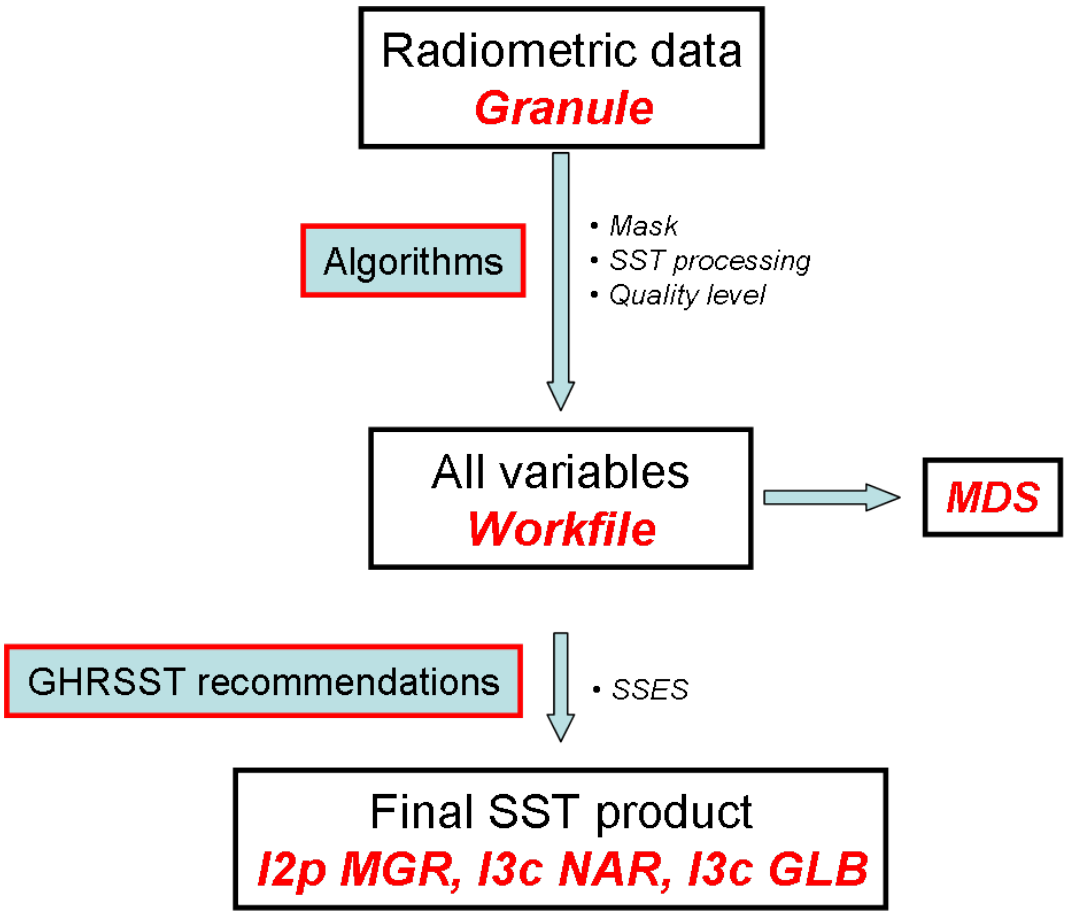

Figure 2: LEO processing chain overview.

2.1 Products

The processing chain treats each granule (equivalent to 3 minutes of acquisition for AVHRR and 1.5 minutes for VIIRS) separately. For each granule, it progressively builds up a workfile (in Netcdf format) containing all information needed (input data, ancillary data) and all variables output at each step of the processing. These workfiles are not distributed; they are the primary finalized output of the chain which will then be used to elaborate the Matchup Dataset (MDS) and the OSI SAF products:

- Level 2 Metop/AVHRR product granule: L2P MGR (MetaGranule) , satellite projection at full resolution (currently for both Metop-B and C)

- Level 3 Metop/AVHRR global: L3C GBL (GloBaL), bi-daily product on a regular grid at 0.05° resolution (currently for Metop-B)
- Level 3 Metop/AVHRR and JPSS/VIIRS North Atlantic Region: L3C NAR, bi-daily product on a stereo-polar grid at 2km resolution (Currently for Metop-B and NOAA-20)

These OSI SAF products are compliant with the recommendation of the GHRSST GDSv2. They are elaborated by extracting the relevant information from the workfiles and by adding necessary information such as the Single Sensor Error Statistics (SSES).

2.2 SST computation in the new LEO processing chain

The LEO processing chains includes a "classical" way of computing SST using a non-linear multi-channel algorithm and a bias correction scheme based on the use of Numerical Weather Prediction (NWP) model and a radiatif transfer model (RTTOV) to simulate brightness temperatures. **The bias correction scheme is used only for Metop/AVHRR processing.**

Figure 3 provides a schematic view of the SST processing in which one can see the two steps mentioned above. The principles are explained below in sections 2.2.2 and 2.2.3 and the details are provided in the section 2.3.

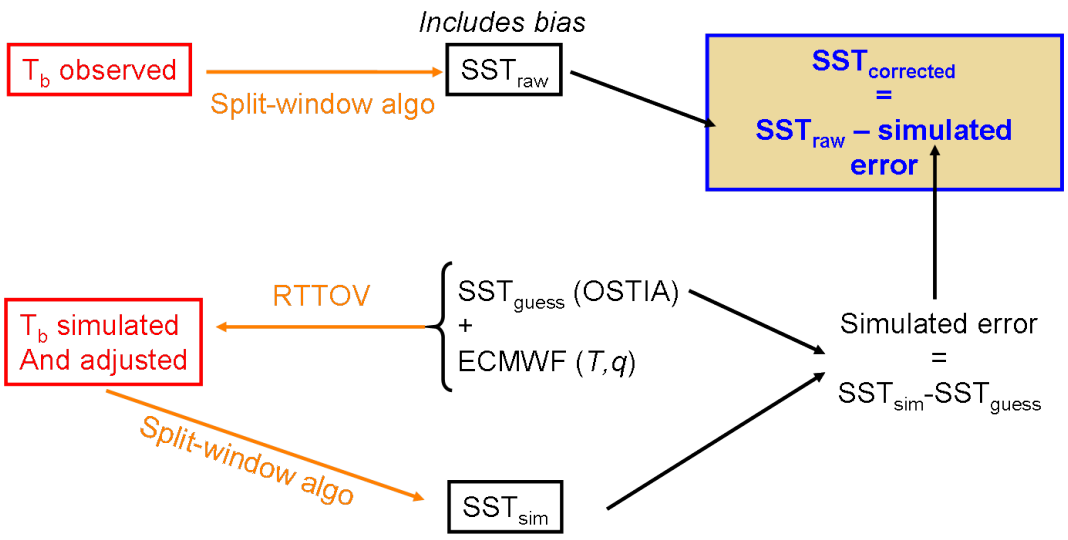

Figure 3: Schematic of the SST processing (including bias correction) in the LEO SST chain.

2.2.1 Land/Lake/Sea/Ice/Cloud mask

The mask to identify land, lake and sea pixels is provided by GMT (Wessel et al., 2013). In the case of Metop/AVHRR it is merged with ARC-Lake database at a resolution of 30" of arc. The cloud mask is provided by MAIA version 4 [RD.1]. These masks are projected onto each granule prior to SST computation.

The sea-ice mask originates from a Bayesian methodology to estimate sea ice probability from the AVHRR and VIIRS radiometric measurements (see section 3.2). This mask is produced for each granule.

2.2.2 The "classical" SST computation

The so-called "classical" SST refers to the SST retrieved by the use of a non-linear split window algorithm to which also include:

- a satellite zenith angle correction computed precisely after launch (ideally during commissioning phase)
- a Saharan Dust Index correction (Merchant et al., 2006a)
- a smoothing of the split window term ($T_{11} - T_{12}$) to reduce radiometric noise impact on SST

In reallity two SST algorithms are defined: one for daytime and one for night-time (see section 3.3 for details). For each pixels, day-time and night-time algorithms are used for sun zenith angle (SZA) below 90°, above 110° respectively. For twilight conditions (sun zenith angle between 90 and 110°) a linear combination of the two algorithms is used. For a given location (pixel) this combination depends on the value of the sun zenith angle and the limit angles of 90 and 110°:

$$\mathrm{SST} = k\,\mathrm{SST}_{\mathrm{day}} + (1-k)\,\mathrm{SST}_{\mathrm{night}} \text{ with } k = \frac{110 - \mathrm{SZA}}{110 - 90} \tag{1}$$

where $\mathrm{SST}_{\mathrm{day}}$ and $\mathrm{SST}_{\mathrm{night}}$ are the SSTs determined by the day-time and night-time algorithm respectively. The factor k is set to 0 and 1 when negative and above 1 respectively.

2.2.3 Bias correction Overview

The "classical" SST computation provides satisfying results. However studies have highlighted regional and seasonal bias due to the inability of the algorithm to cope with a wide range of atmospheric water content.

The bias correction method used in the LEO processing chain (Le Borgne et al., 2011), makes use of an atmospheric RTM forced with the temperature and water vapour atmospheric profiles from a NWP model and an initial guess SST to estimate an algorithm correction. Simulations of BTs are performed for all clear sky pixels. An adjustment is made to the simulated BTs to take into account potential uncertainties originating from the RTM, the atmospheric profiles from the NWP model and the instrument filter functions. A "simulated" SST is then computed using the non-linear algorithm used for computation of "classical" SST (see section 3.3). Under some hypothesis and strict selection, the difference between the "simulated SST" and the guess SST is considered to be the algorithm correction which is then added to the "classical" SST.

2.3 Quality level and test indicators

An important step of the processing is to control the cloud mask. It consists in a series of tests designed to identify pixels contaminated by undetected clouds or atmospheric dust aerosols for instance. We use the concept of indicator to quantify, in an empirical way, the risk of having a significant error in the SST retrieval. For each test, the tested quantity (tested_value) is compared to a limit value (limit_value) and to a critical value (critical_value). Outside this range there is either no problem or the risk of error is too high. The core definition of the test indicator is given below, however many other factors can influence each indicators (for example availability of ancillary data used in the definition of the indicator) that are not detailed here:

$$\mathrm{test_indicator} = 100(\mathrm{tested_value} - \mathrm{limit_value})/(\mathrm{critical_value} - \mathrm{limit_value}) \tag{2}$$

There is a range of test_value, for example: the difference between the climatological SST and the retrieved SST, the SDI, the distance to cloud, etc. [limit_value, critical_value] define a range of the test_value below and above which the test_indicator is 0 and 100 respectively.

The formulation above has the advantage of homogenising all the indicators on a unique scale:

- 0: no problem
- $]0, 100[$: potential problem
- 100: critical problem

There are two types of indicators: (i) the common indicators, independent of the SST retrieved and the algorithm used, they are generic to the whole processing. They include the dust indicator, the distance to cloud indicator and the ice indicator. (ii) The specific indicators, based on the value of the SST retrieved in comparison to climatologies of SST and SST gradients (the SST value indicator and the SST gradient indicator). At the end of the processing all these indicators are combined into one single indicator by means of a weighted average: this is the SST mask indicator.

Two other indicators are defined that do not enter in the SST mask indicator, but are considered for determining the quality level: the indicator reflecting the uncertainties of the SST algorithm with respect to the satellite zenith angle (algorithm indicator), and the indicator about the confidence we have in the correction term (the SST correction indicator).

A brief description of the tests is given in table 2:

Table 2: List of indicators contributing to the quality level

Test	**Description/purpose**
SST value	This test aims at attributing a lower quality level to SST values too different from climatology. The local value of estimated SST is compared to a climatology of SST, the larger the difference between estimated SST and SST climatology, the higher the indicator.
SST spatial variability	The main objective of this test is to attribute a lower quality level to pixels in areas where the gradients are unrealistically large due to the presence of undetected cloud cover in most cases. The local value of the SST gradient is compared to a climatology of maximum gradient.
Aerosol dust	This test influences the quality level of pixels contaminated by Saharan dusts. It is directly related to the either the Aerosol Optical Depth or the Saharan Dust Index.
Distance to cloud	Pixels in the immediate vicinity of clouds are likely to be partly covered by cloud or affected by transparent undetected clouds.
Sea ice	The purpose of this test is to degrade the quality of pixels suspected to contain ice.
Satellite zenith angle	The test takes into account the fact that high satellite zenith angle is likely to lead to higher uncertainty because of higher atmospheric optical depth. The resulting indicator is directly linked to the satellite zenith angle.
SST correction	This test is based on the assumption that high SST corrections are associated with high uncertainties. It is directly linked to the value of the SST correction. It is only applied in the algorithm correction method.

Quality levels are designed to help users to filter out data that are not sufficiently good for their applications. It is essential to adopt the recommendation of the GHRSST formalised through the GDS v2 document. For infrared derived SST six quality levels are defined. 0: unprocessed; 1: cloudy, 2: bad, 3: suspect, 4 acceptable, 5 excellent.

The value of the quality level is determined by examining the values of three indicators: the SST mask indicator (resulting from several sub-indicators as explained above), the algorithm indicator and the SST correction indicator (only in the case of the algorithm correction method, see section 3.5). The poorest indicator will drive the value of the quality level.

2.4 Sensor Specific Error Statistics (SSES)

The SSES are observational error estimates provided at pixel level as a bias and standard deviation as per GHRSST GDSv2 requirements.

The SSES bias and standard deviation (given in Table 3 and 4) are calculated for each quality level from analysing differences between full resolution satellite SSTs collocated with drifting buoys available on operational matchup data set. For more information about how this dataset is constructed, please refer to section 5.1. In Table 3 and 4, SSES for twilight condition are computed as the average between daytime and nighttime SSES.

We apply a quality control on drifting buoys: buoy SSTs are checked to be within 5 K of climatology and we also use the buoys blacklist build in M-F/CMS and delivered by OSI SAF to eliminate erroneous measurements.

Table 3: SSES for METOP-B SST

	Quality level	**SSES bias [K]**	**SSES STD [K]**
Daytime	2	-1.80	1.88
	3	-0.21	0.50
	4	-0.06	0.43
	5	-0.01	0.34
Twilight	2	-2.58	1.99
	3	-0.28	0.52
	4	-0.07	0.43
	5	-0.00	0.33
Night-time	2	-3.35	2.10
	3	-0.37	0.54
	4	-0.08	0.42
	5	0.01	0.31

Table 4: SSES for METOP-C SST

	Quality level	SSES bias [K]	SSES STD [K]
Daytime	2	-1.61	1.65
	3	-0.15	0.67
	4	-0.04	0.57
	5	0.03	0.48
Twilight	2	-2.16	1.63
	3	-0.22	0.67
	4	-0.08	0.55
	5	-0.01	0.44
Night-time	2	-2.71	1.62
	3	-0.29	0.66
	4	-0.13	0.53
	5	-0.00	0.40

2.5 Ancillary data

Table 5 lists all data needed for the processing of SST by the new LEO processing chain for Metop/AVHHR and JPSS/VIIRS.

Table 5: List of ancillary data needed

Parameter	Source	Use
Land/Sea/Lake mask	GMT (Wessel et al., 2013) and ARC-Lake (only for Metop processing)	Identify pixels candidate to processing
Cloud Mask	MAIA v4 [RD.1]	Mask cloudy pixels and backup for ice detection
Foundation SST	OSTIA	Guess SST for simulation of BTs
Foundation SST climatology	OSTIA	Used to degrade quality level of pixels strongly deviating from climatology
Saharan Dust Index	SEVIRI OSI SAF processing	Used to apply correction to estimated SST affected by Saharan dusts
Air humidity (q) and temperature (T)	ECMWF prevision	Input for simulation of BTs by the radiative transfer model RTTOV
Aerosol Optical Depth	NAAPS	Replace SDI information where missing (outside MSG/SEVIRI disk for example)
Maximum ice extent	NSIDC	Used to determine were to apply the ice detection method
Ice edge	OSI SAF	Backup in the event of ice detection method failure

3 Low Earth Orbiter processing chain algorithms descriptions

This section describes all the algorithms and methods used in the new LEO processing chain to produce SST corrected from regional and seasonal bias.

3.1 Saharan Dust Index (SDI)

The impact of the presence of Saharan dusts on brightness temperature at the wavelength used for determining SST is known for a long time. We use the SDI developed by Merchant et al. (2006a) for MSG/SEVIRI in order to compute an empirical correction for SST retrievals affected by Saharan dusts.

The SDI computation has originally been developed from nighttime MSG/SEVIRI 3.9, 8.7, 10.8 and 12.0μm channels. An extension for daytime (Merchant et al., 2006b) was implemented in 2012. The information on the SDI is only available for MSG/SEVIRI disk, outside this area, the Navy Aerosol Analysis and Prediction System (NAAPS) model output of dust AOD is used to degrade the quality level if needed since no correction is possible.

3.2 Ice detection algorithm

Pixels containing ice need to be masked or at least the quality level needs to be degraded in the case of low sea ice concentration (partial sea ice coverage). At high latitude it can be difficult to distinguish between water, sea ice and cloud.

A Bayesian method is used to estimate the probability of having water, ice and cloud in each pixel. During daytime and twilight three spectral features of the instruments are used:

- The ratio between Channel 2 to Channel 1
- The ratio between Channel 3 to Channel 1
- The difference between brightness temperature at 3.7 and 11μm (when 3.7μm is available, i.e. twilight conditions)

For nighttime only the difference between brightness temperature at 3.7 and 12μm is used.

An a priori knowledge of the Gaussian probability distribution functions for the features listed above given each of the three classes (ice, water and cloud) is required. A complete description of the methodology can be found in the [RD.2].

3.3 SST algorithms

In this section we present the "classical" SST algorithm, the method for bias correction of SST based on simulation of BTs (only used for AVHRR processing at the moment), and the method used for taking into account atmospheric Saharan dust contamination.

3.4 Non-linear SST algorithm

The algorithms for computing SST from radiometric measurements in the infrared domain are called "split-window" algorithms because they take advantage of the difference in the sensitivity to atmospheric effects between infrared channels at 11 and 12μm for instance. They are widely used and many versions have been developed for various instruments and conditions of use. These algorithms have the following generic form:

$$\hat{\mathrm{x}} = a_0 + \mathbf{a}^\top \mathbf{y}_0 \tag{3}$$

Table 6: Coefficient of the algorithm for Metop-B/AVHRR.

	a	b	c	d	e	f	g
Day	0.99786	0.01477	0.63476	0.42829	0.05108	0.49974	0.94919
Night	1.00838	0.03141	0.75499	0.29129	1.12360	0.99763	

Table 7: Coefficient of the algorithm for Metop-C/AVHRR.

	a	b	c	d	e	f	g
Day	0.95685	0	0	0.47807	0.05421	1.570075	0.85599
Night	1.00614	0.01801	0.61859	0.27091	1.15315	1.09370	

where, $\hat{x}$ is the estimated SST, a_0 is an offset coefficient, $\mathbf{a}$ is a column vector of weighting coefficients and $\mathbf{y}_0$ contains the observed BTs. The coefficients contained in the vector $\mathbf{a}$ are potentially functions of SST climatology and satellite zenith angle.

A classical non-linear SST algorithm will be used to provide the "classical" SST which is:

- used in the calculation of an initial value of some indicators and QL (see section 2.3).
- used in the brightness temperature adjustment step (see section 3.5.2)
- the basis of the algorithm correction method (see section 3.5.3)

The form of the algorithm is the same for Metop/AVHRR and JPSS/VIIRS processing and is given by equations 4 and 5:

$$\mathrm{SST}_{\mathrm{day}} = (a + b\,S_\Theta)\,T_{11} + (c + d\,S_\Theta + e\,T_{clim})(T_{11} - T_{12}) + f + g\,S_\Theta \quad (4)$$

$$\mathrm{SST}_{\mathrm{night}} = (a + b\,S_\Theta)\,T_{37} + (c + d\,S_\Theta)(T_{11} - T_{12}) + e + f\,S_\Theta \quad (5)$$

where T_{37}, T_{11} and T_{12} are the observed brightness temperature at the central wavelength of around 3.7, 10.8 and 12.0μm respectively for each instrument, $S_\Theta = sec(\Theta) - 1$ and Θ is the satellite zenith angle. T_{clim} is the climatological sea surface temperature.

The parameters of equations 4 and 5 are determined by regression using simulation of BTs computed on a dataset of atmospheric profiles from NWP model using RTTOV radiative transfer model. This step is generally performed before launch as soon as the filter function of the instrument are known to us. As input to RTTOV we use the short range forecast of ECMWF. In total 102693 profiles are used and simulations of BTs are done for secant of the satellite zenith angle ranging from 1 to 3.25 with a step of 0.25. This results in 716618 simulations of BTs for day and night with which we perform a regression to estimate the coefficients of the algorithms.

A second step consists in adjusting the last two parameters of the equations (f and g in equation 4 and e and f in equation 5) using drifting buoys measurements. This step is generally done when enough collocation data (between satellite and drifting buoys) have been collected, typically at least a few month.

The values of the coefficients are given in tables 6,7 and 8 for AVHRR and VIIRS respectively.

The term $(T_{11} - T_{12})$ in equations 4 and 5 is used in this "split-window" algorithms to correct for absorption by water vapour in the atmosphere. However, this term is also particularly sensitive to radiometric noise; it is therefore smoothed over boxes (of a size 11x11 pixels in which the atmosphere is assumed to be homogeneous) by a simple average, applied to clear/no ice pixels. This classical procedure reduces the noise in the retrieved SST.

Table 8: Coefficient of the algorithm for NOAA-20/VIIRS.

	a	b	c	d	e	f	g
Day	1.01266	0.02548	1.26302	0.44245	0.02631	1.03315	0.99571
Night	1.00867	0.02645	1.06332	0.30209	0.91770	0.64854	

Since the coefficient of the SST algorithm are established using simulations from RTTOV radiative transfer model and de-biased against drifting buoys measurements (at a depth of 20 to 30 cm), the retrieved SST is considered to be the sub-skin SST. One could apply a $-0.17°$C (Donlon et al., 2002) to get the skin SST. However this offset is only a very rough conversion term valid at large scale for wind speed generally exceeding $6\,\mathrm{m/s^{-1}}$.

3.5 Bias correction

This section describes the bias correction method Le Borgne et al. (2011) and the way it has been implemented in the context of the new LEO processing chain.

Important note: The bias correction procedure is only used in the processing of Metop/AVHRR SST. It is not used for JPSS/VIIRS processing.

3.5.1 Simulation of brightness temperature

The RTM used for these simulations is RTTOV version 11. RTTOV is a fast radiative transfer model designed for passive visible, infrared and microwave satellite radiometers, spectrometers and interferometers. The code of RTTOV is in FORTRAN-90 and enables a great number of simulations in a reasonable time (note that the dimension of each granule, corresponding to 3 minutes of acquisition of METOP/AVHRR, is 1080x2048 pixels). RTTOV simulates the top of atmosphere radiances for a large number of satellite sensor given:

- Atmospheric profile of water vapour and optionally other trace gases
- Satellite and solar zenith angles
- Surface temperature, pressure and optionally emissivity and reflectance

For more information about RTTOV, the reader is referred to [RD.3] and [RD.4]. In our case, RTTOV is used to simulate clear-sky (i.e. no cloud and no aerosols) BTs at 3.7, 10.8 and 12.0μm.

In order to perform the simulations of BTs, we need to have a priori knowledge of the SST and the Lake Water Surface temperature (LWST) for each pixel; this is what we call the guess SST. This information is extracted from the Operational Sea Surface Temperature and Sea Ice Analysis (OSTIA, Donlon et al. (2012)) and ARC-Lake v1 for lake surface water temperature (MacCallum and Merchant, 2012) for which OSTIA does not provide information. Both datasets are available on a regular grid at the resolution of 0.05° for OSTIA and 30" for ARC-Lake. These data are reprojected onto each granule directly.

OSTIA and ARC-Lake SSTs are foundation temperature. We need to convert this into sub-skin SST for comparison with retrieved SST. This is done by filtering out cases of strong temperature gradient near the surface by setting conditions (see section 3.5.2) on minimum wind speed to insure proper mixing of the surface water. A further conversion skin SST is required for use in RTTOV. To do this we apply a skin-to-sub-skin correction of 0.17°C (Donlon et al., 2002). Please note that this correction is mostly valid at wind speed higher than 6 m/s.

Knowledge of the atmospheric profile of temperature water vapour comes from ECMWF NWP model. It is operationally available at Météo-France at a time step of 3 hours and on a

regular grid at 0.5° of resolution. These data are first interpolated onto the OSTIA grid using a bilinear interpolation method. There is no interpolation in time; we use the nearest output available at processing time.

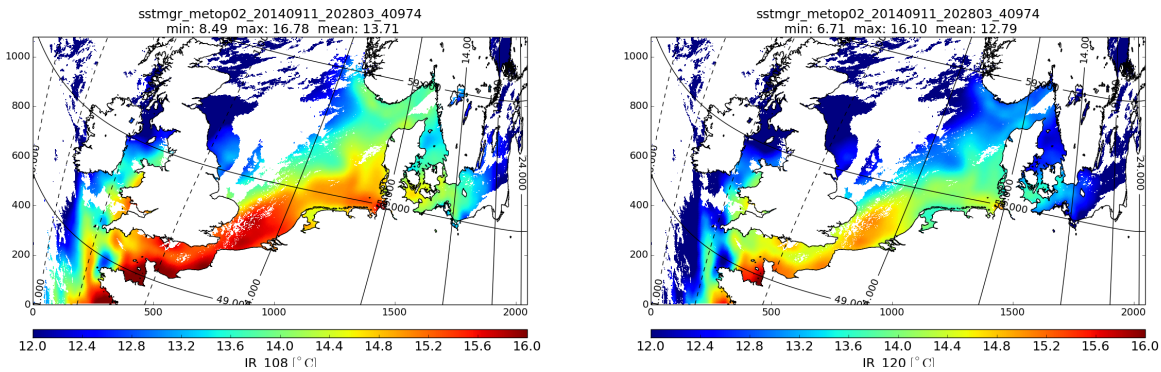

Figure 4: RTTOV simulations of brightness temperature for 10.8 and 12.0μm for a sample granule.

Figure 4 shows a sample a Bt simulations for 10.8 and 12.0μm channels performed on all clear sky pixels of a Metop/AVHRR granule.

3.5.2 Adjustment of the BTs

Simulated BTs are different than the observations. The purpose of the adjustment phase is to correct for systematic differences between observed and simulated BTs due to:

- ECMWF water vapour profiles uncertainties
- Profile sampling
- RTTOV uncertainties
- AVHRR filter function and calibration uncertainties

The only reference we have to do the adjustment is the set of observations (satellite BTs). In a synthetic way, we use the difference between simulations and observations (spatially and temporally smoothed) and interpret the differences as a correction. However, the risk is to make the simulated BTs to match too closely the observed BTs. This would defeat the purpose of an adjustment. The description of the BT adjustment method is provided in detailed in Tomažić et al. (2014).

The major hypothesis we make here is that there is no average bias between the guess SST (used in BTs simulation) and the true SST. It is therefore crucial to properly filter out cases (pixels) where the simulated SST cannot be compared with guess SST (for example if there is a diurnal cycle or cloud contamination). This is done through several steps of filtering:

1. Quality level filtering: only good quality SST retrievals are used (QL $\geq$ 3, see section 2.3).
2. Dust aerosol filtering: based on the dust indicator.
3. SST filtering: we ensure that "classical SST" and guess SST are close to each other (less than 1K difference)
4. BT simulation filter removes cases where simulations clearly failed:

- For the 3.7μm channel: $|T_{37}^{sim} - T_{37}^{obs}| \leq 1.5$K
- For the 10.8 and 12.0μm channel: $|T_{11}^{sim} - T_{11}^{obs}| \leq 1.5$K

5. Algorithm related filters based on solar zenith angle (Θ_{sol}) and wind speed at 10 meters (u_{10}) to eliminate cases of diurnal warming. The filter is different for latitude above 60°N.

   - For the 3.7μm channel:
     If latitude > 60°N: $\Theta_{sol} \geq 110°$ and $|T_{37}^{sim} - T_{37}^{obs}| \leq 0.5$K
     If latitude $\leq$ 60°N: $\Theta_{sol} \geq 110°$ and $u_{10} \geq 4\text{ms}^{-1}$
   - For the 10.8 and 12.0μm channel:
     If latitude > 60°N: ($\Theta_{sol} < 110°$ and $u_{10} \geq 10\text{ms}^{-1}$) or ($\Theta_{sol} \geq 110°$ and $|T_{11}^{sim} - T_{11}^{obs}| \leq 0.5$K)
     If latitude $\leq$ 60°N: $\Theta_{sol} \geq 90°$ and $u_{10} \geq 4\text{ms}^{-1}$

Once the selection based on the above filtering is done for all the granules of the past three days, data are gridded into a 3-dimensional array of dimensions (6 slots, 360, 180) which is a stack of six global grid (cell size of $1 \times 1°$) each corresponding to a 12hour period over the pas three days. Each grid cell is filled in with the best quality value falling in that cell during the last three days. There is one 3-dimensional array for each channel.

The data contained in the 3-dimensional arrays are used to produce three functions (δ_{sec}) of satellite zenith angle secant dependency of the difference between simulated and observed BTs ($\Delta BT = T_b^{sim} - T_b^{obs}$). These functions are called the normalisation functions and are used to normalise the ΔBTs: $\Delta BT_{norm} = \Delta BT - \delta_{sec}(\Theta_s)$.

The normalisation function is of the following form: $\delta_{sec}(\Theta_s) = a\, sec(\Theta_s)^2 + b\, sec(\Theta_s) + c$ where a, b and c are found by regression over the filtered BTs for each channel separately.

The normalisation is applied to each 3-dimensional array. They are then averaged in time to produce 2-dimensional fields of the normalised correction at $1 \times 1°$ resolution. These fields are smoothed out in order to fill in any gap. The radius of smoothing is 15° and requires 25 valid data minimum. The smoothing is repeated until all gaps are filled in.

Note that, to the North of 60°N and to the South of 60°S, the 2-dimensional grid is filled in with the mean values of all existing data in these very high and low latitude respectively. Because in these region very few data are available due to the strict filtering described above (in particular the conditions on the solar zenith angle), the adjustment can have a negative impact. Tests have shown that results obtained with a fixed value of adjustment were better than those obtained with dynamic adjustment.

The fields are then interpolated onto a 0.05° resolution regular grid (corresponding to the OSTIA grid and to the global OSI SAF SST product grid) by bilinear interpolation.

The AD (Adjustment Dataset) is constituted by the adjustment grid and the set of parameters of the normalisation function. In an operational framework one AD is built every 12 hours.

When a granule is processed, the nearest AD in time is used: the 2-dimensional fields of normalised adjustments are projected onto the granule and added to the simulated BTs, a correction depending on the satellite zenith angle secant is then applied by using the normalisation function. This results in the adjusted simulated BTs. Figure 5 shows an example of BT adjustment at 0h on the 5th of November 2014.

3.5.3 Corrected SST

The method of algorithm correction was developed by Le Borgne et al. (2011), it is used today in the operational processing of OSI SAF SST products from Metop-B and MSG/SEVIRI. Operational SST delivered in those products is the corrected SST.

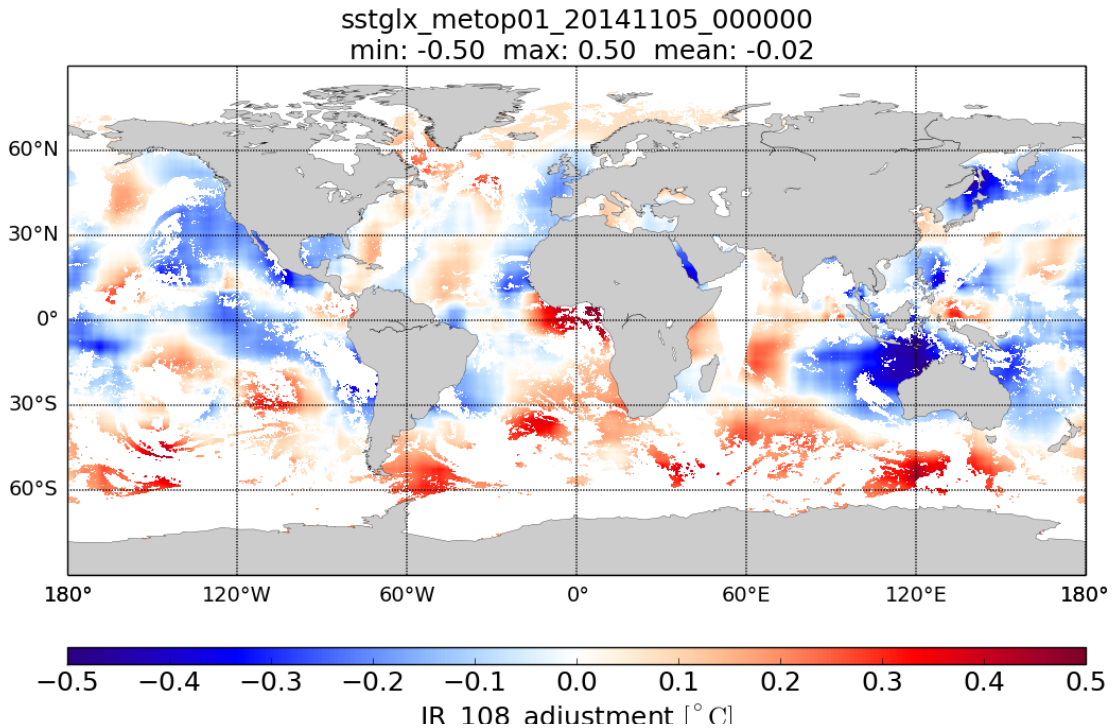

Figure 5: Sample global BT adjustment field for 10.8μm channel.

Once simulated BTs have been adjusted, as explained above, a "simulated" SST is produced by applying the SST algorithm described in section 3.4. In this computation, the SDI correction is not applied since only SDI-free cases have been simulated. Similarly, we do not apply the smoothing on the (T11-T12) since its purpose is to correct for radiometric noise effect which does not exists in simulated BTs.

The following difference is then computed:

$$\Delta SST = SST^{sim} - SST^{guess} \tag{6}$$

Since the BT simulations used to compute SST^{sim} have been adjusted to correct for uncertainties linked with RTTOV and atmospheric water vapour profiles, ΔSST represent the error due to the algorithm which is unable to cope with all atmospheric conditions.

The corrected SST (SST^{cor}) is then computed as follow:

$$SST^{cor} = SST^{obs} - \Delta SST \tag{7}$$

where SST^{obs} is the "classical" SST as computed by the algorithm presented in section 3.4.

Figure 6 shows the observed difference of the "classical" SST to the guess SST (top), it displays some obvious regional biases: for instance a strong negative bias over the Gulf of Guinea, and a positive one along the South West coast of North America. The same patterns are observed in the simulated difference, or the average estimated algorithm uncertainty (Figure 6, bottom). The corrected SST is computed by subtracting the algorithm error to the "classical" SST.

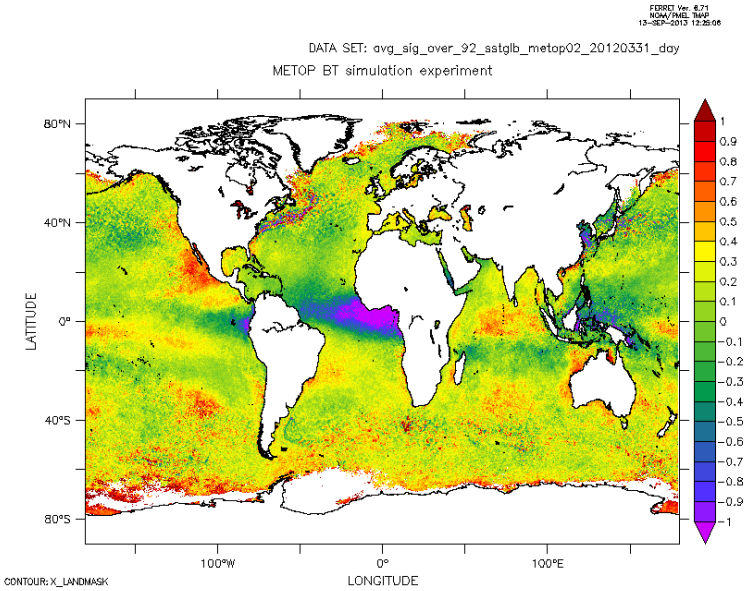

errsst (K)

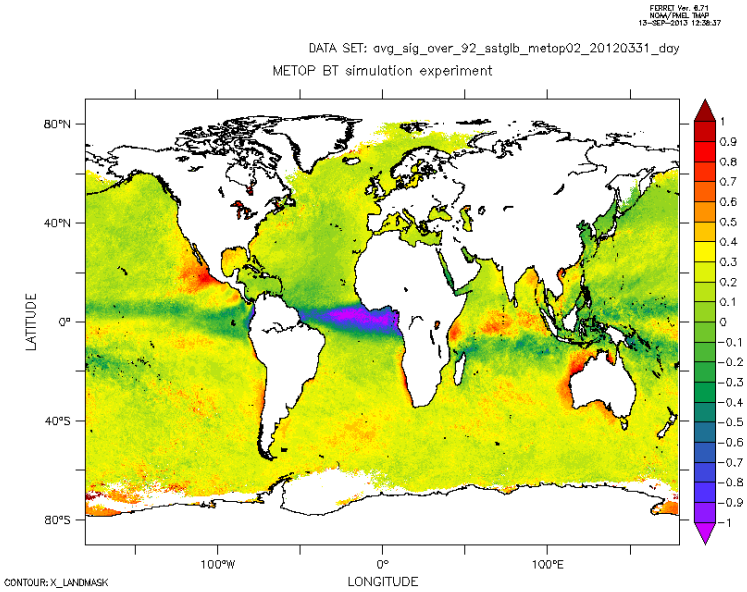

−1*AVG_CORSST

Figure 6: Average (JFM 2012) difference between "classical" SST and guess SST (top), and difference between "simulated" SST and guess SST (bottom), this is the predicted SST uncertainty or average estimated algorithm uncertainty. Note that these results have been obtained for Metop-A/AVHRR.

4 SST temporal synthesis

OSI-201-b (Global Metop SST) and OSI-202-c (North Atlantic Regional SST) products are gridded product temporally composited during 12 hours and 6 hours respectively.

SST is computed for every Metop/AVHRR and JPSS/VIIRS granule received. To build the composites, the intermediate primary workfiles resulting are to be re-mapped onto a regular 0.05° grid (OSI-201-b) or a 2km stereo-polar grid (OSI-202-c).

For the OSI-201-b and OSI-202-c products, during the operational processing four global grids, each corresponding to a quality level (2,3,4 and 5), are populated as the granules are processed. The method used is a nearest neighbour with a ad hoc search radius. At the end of the compositing period 12 hours the four global grid are concatenated into one global field giving priority to the best quality level.

5 Validation procedure

The validation consists in assessing the estimated SST against a reference which we consider thrustworthy. For the purpose of validation, we built a colocation dataset (the Matchup Dataset, MDS) which contains all the needed information.

5.1 The Matchup Dataset

All validation procedures require a MDS has been elaborated. In an operational prospective, the MDS gathers in situ SST measurements from ship, moored buoys and drifting buoys available through the Global Telecommunication System (GTS). Collocated full resolution satellite information is added in a 3 hours time frame around the measurement. It consists of all the variables included in the granule workfile extracted in a 21×21 box around the measurements. The MDS for day d is elaborated with a five days delay (d+5) to ensure all in situ data are available through GTS.

For the purpose of operational validation:

- Only drifter and moored buoys are considered
- Only the central SST of each box is used
- Nighttime and daytime SST are validated separately

5.2 Validation results

Basic statistics are computed such as mean and standard deviation (STD) of the differences between the retrieved SST and the measurements are computed and graphics are produce:

- Globally and regionally
- On a map through a binning process (on a regular grid and for a time frame).
- For different selection criteria, for example based on the quality level or wind speed, etc...
- Against different variables: latitude, SDI, satellite zenith angle, etc... as plots of the average difference and STD

Validation results are available in the validation reports [RD.5] and [RD.6] for AVHRR and VIIRS SST products. Operational NRT validation results are available on the OSI SAF website http://osi-saf.eumetsat.int.

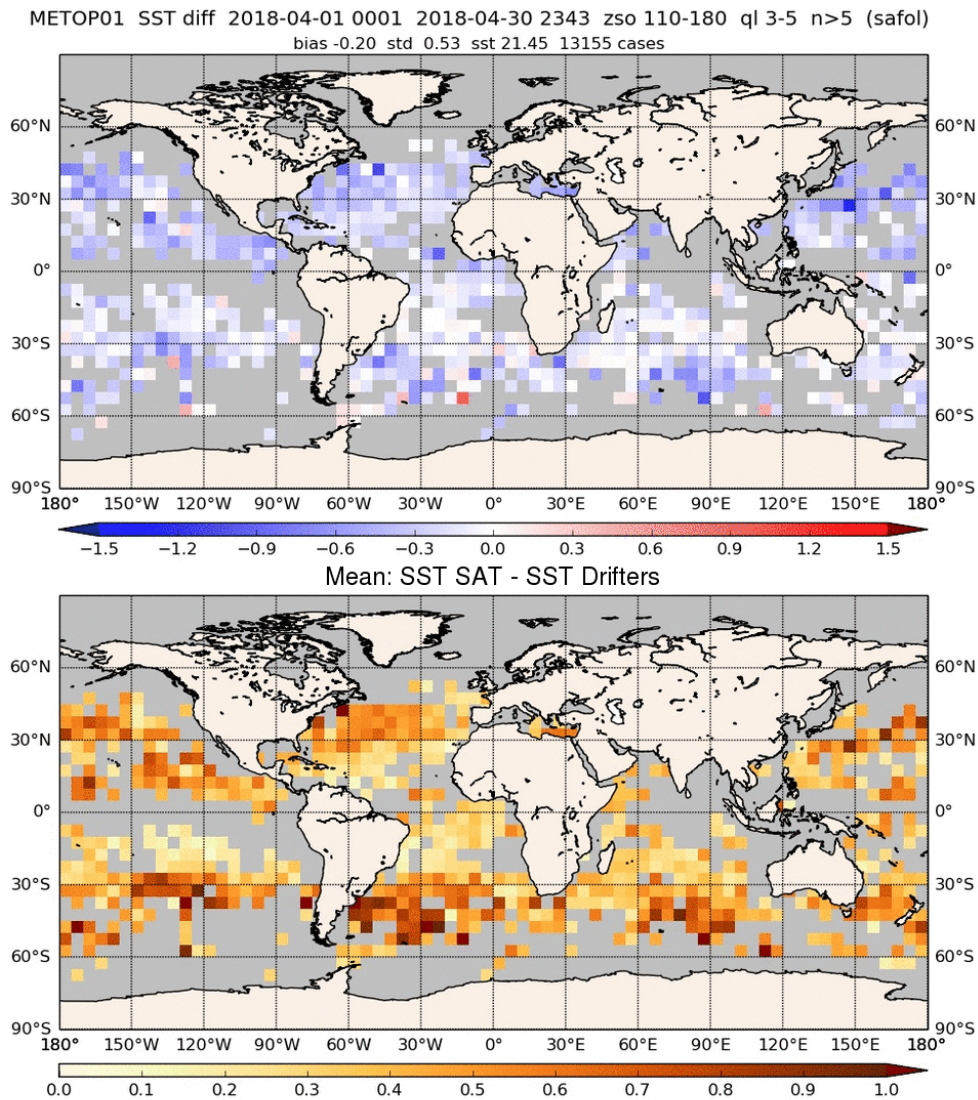

Figure 7: Sample of the routine validation maps that can be found on http://osi-saf.eumetsat.int. Monthly map of the mean bias (top) and standard deviation (bottom) of satellite SST minus drifting buoys temperature measurement, April 2018.

References

Donlon, C. J., Martin, M., Stark, J., Roberts-Jones, J., Fiedler, E., and Wimmer, W. (2012). The operational sea surface temperature and sea ice analysis (OSTIA) system. *Remote Sensing of Environment*, 116:140—-158.

Donlon, C. J., Minnett, P. J., Gentemann, C., Nightingale, T. J., Barton, I. J., Ward, B., and Murray, M. J. (2002). Toward improved and validation of satellite and sea surface and skin temperature and measurements and for climate and research. *Journal of Climate*, 15:353–359.

Le Borgne, P., Legendre, G., and Péré, S. (2012). Comparison of MSG/SEVIRI and drifting buoy derived diurnal warming estimates. *Remote Sensing of Environment*, 124:622–626.

Le Borgne, P., Roquet, H., and Merchant, C. (2011). Estimation of sea surface temperature

from the spinning enhanced visible and infrared imager, improved using numerical weather prediction. *Remote Sensing of Environment*, 115(1):55–65.

McCain, E. P., Pichel, W. G., and Walton, C. C. (1985). Comparative performance of AVHRR-based multichannel sea surface temperature. *Journal of Geophysical Research*, 90:11587–11601.

Merchant, C. J., Embury, O., Le Borgne, P., and Bellec, B. (2006a). Saharan dust in nighttime thermal imagery: Detection and reduction of related biases in retrieved sea surface temperature. *Remote Sensing of Environment*, 104(1):15–30.

Merchant, C. J., Filipiak, M. J., Le Borgne, P., Roquet, H., Autret, E., Piollé, J.-F., and Lavender, S. (2008). Diurnal warm-layer events in the western mediterranean and European shelf seas. *Geophys. Res. Lett.*, 35(4):1–4.

Merchant, C. J., Harris, A. R., Roquet, H., and Le Borgne, P. (2009). Retrieval characteristics of non-linear sea surface temperature from the advanced very high resolution radiometer. *Geophys. Res. Lett.*, 36(17):1–5.

Merchant, C. J., Horrocks, L. A., Eyre, J. R., and O'Carroll, A. G. (2006b). Retrievals of sea surface temperature from infrared imagery: origin and form of systematic errors. *Quarterly Journal of the Royal Meteorological Society*, 132(617):1205–1223.

Tomažić, I., Le Borgne, P., and Roquet, H. (2014). Assessing the impact of brightness temperature simulation adjustment conditions in correcting Metop-A SST over the mediterranean sea. *Remote Sensing of Environment*, 146:214–233.

Walton, C. C., Pichel, W. G., Sapper, J. F., and May, D. A. (1998). The development and operational application of nonlinear algorithms for the measurement of sea surface temperatures with the NOAA polar-orbiting environmental satellites. *Journal of Geophysical Research*, 103:27999–28012.

Wessel, P., Smith, W. H. F., Scharroo, R., Luis, J. F., and Wobbe, F. (2013). Generic mapping tools: Improved version released. *Eos, Transactions, American Geophysical Union (EOS)*, 94:409–410.